

An extended cavity diode-pumped femtosecond Yb:KGW laser for applications in optical DNA sensor technology based on fluorescence lifetime measurements

Arkady Major and Virginijus Barzda

Department of Physics and Institute for Optical Sciences, University of Toronto, 3359 Mississauga Rd. N.,
Mississauga, ON, L5L 1C6, Canada
a.major@utoronto.ca

Paul A. E. Piunno, Sergei Musikhin, and Ulrich J. Krull

Department of Chemical and Physical Sciences, University of Toronto at Mississauga, 3359 Mississauga Rd. N.,
Mississauga, ON, L5L 1C6, Canada
ppiunno@utm.utoronto.ca

Abstract: A reliable and power-scalable extended cavity diode-pumped passively mode-locked Yb:KGW laser generating ~200 fs long pulses at a repetition rate of 15 MHz was developed and characterized. The laser delivered up to 150 mW of average power at fundamental wavelength of 1040 nm, corresponding to a pulse energy of 10 nJ. The laser radiation was frequency-doubled in a single pass configuration within a nonlinear BIBO crystal to produce femtosecond green radiation at 520 nm with peak power of ~200 W. The generated second harmonic served as an excitation source for an optical DNA biosensor based on fluorescence lifetime measurements obtained using the time-correlated single photon counting technique.

© 2006 Optical Society of America

OCIS Codes: (140.3580) Lasers, solid-state; (140.3480) Lasers, diode-pumped; (140.7090) Ultrafast lasers; (140.4050) Mode-locked lasers

References and links

1. J. H. Watterson, S. Raha, C. C. Kotoris, C. C. Wust, F. Gharabaghi, S. C. Jantzi, N. K. Haynes, N. H. Gendron, U. J. Krull, A. E. Mackenzie and P. A. E. Piunno, "Rapid detection of single nucleotide polymorphisms associated with spinal muscular atrophy by use of a reusable fibre-optic biosensor," *Nucl. Acids Res.* **32**, e18 (2004).
2. P. A. E. Piunno and U. J. Krull, "Trends in the development of nucleic acid biosensors for medical diagnostics," *Anal. Bioanal. Chem.* **381**, 1004-1011 (2005).
3. J. Olmsted and D. R. Kearns, "Mechanism of ethidium bromide fluorescence enhancement on binding to nucleic acids," *Biochem.* **16**, 3647-3654 (1977).
4. R. Paschotta, J. Aus der Au, G. J. Spühler, F. Morier-Genoud, R. Hövel, M. Moser, S. Erhard, M. Karszewski, A. Giesen, and U. Keller, "Diode-pumped passively mode-locked lasers with high average power," *Appl. Phys. B* **70**, S25-S31 (2000).
5. M. Ramaswamy, M. Ulman, J. Paye, and J. G. Fujimoto, "Cavity-dumped femtosecond Kerr-lens mode-locked Ti:A1₂O₃ laser," *Opt. Lett.* **18**, 1822-1824 (1993).
6. A. Killi, A. Steinmann, J. Dörring, U. Morgner, M. J. Lederer, D. Kopf, and C. Fallnich, "High-peak-power pulses from a cavity-dumped Yb:KY(WO₄)₂ oscillator," *Opt. Lett.* **30**, 1891-1893 (2005).
7. N. H. Schiller, X. M. Zhao, X. C. Liang, L. M. Wang, and R. R. Alfano, "Compact picosecond Nd:glass mode-locked laser with variable cavity length from 5 to 21 m," *Appl. Opt.* **28**, 946-948 (1989).
8. A. R. Libertun, R. Shelton, H. C. Kapteyn, and M. M. Murnane, "A 36 nJ-15.5 MHz extended-cavity Ti:sapphire oscillator," in *Conference on Lasers and Electro-Optics*, OSA Technical Digest (Optical Society of America, Washington DC, 1999), paper CThR3, pp. 469-470.

9. A. M. Kowalevich Jr., A. Tucay Zare, F. X. Kärtner, J. G. Fujimoto, S. Dewald, U. Morgner, V. Scheuer and G. Angelow, "Generation of 150-nJ pulses from a multiple-pass cavity Kerr-lens mode-locked Ti:Al₂O₃ oscillator," *Opt. Lett.* **28**, 1597-1599 (2003).
10. V. Shcheslavskiy, V. V. Yakovlev, A. Ivanov, "High-energy self-starting femtosecond Cr⁴⁺:Mg₂SiO₄ oscillator operating at a low repetition rate," *Opt. Lett.* **26**, 1999-2001 (2001).
11. R. P. Prasankumar, Y. Hirakawa, A. M. Kowalevich Jr., F. X. Kaertner, and J. G. Fujimoto, "An extended cavity femtosecond Cr:LiSAF laser pumped by low cost diode lasers," *Opt. Express* **11**, 1265-1269 (2003).
12. V. Z. Kolev, M. J. Lederer, B. Luther-Davies, and A. V. Rode, "Passive mode locking of a Nd:YVO₄ laser with an extra-long optical resonator," *Opt. Lett.* **28**, 1275-1277 (2003).
13. D. N. Papadopoulos, S. Forget, M. Delaigue, F. Druon, F. Balembois, and P. Georges, "Passively mode-locked diode-pumped Nd:YVO₄ oscillator operating at an ultralow repetition rate," *Opt. Lett.* **28**, 1838-1840 (2003).
14. G. I. Petrov, V. V. Yakovlev, N. I. Minkovski, "Broadband nonlinear optical conversion of a high-energy diode-pumped picosecond laser," *Opt. Commun.* **229**, 441-445 (2004).
15. N. V. Kuleshov, A. A. Lagatsky, A. V. Podlipensky, V. P. Mikhailov, G. Huber, "Pulsed laser operation of Yb-doped KY(WO₄)₂ and KGd(WO₄)₂," *Opt. Lett.* **22**, 1317-1319 (1997).
16. S. L  v  que-Fort, D. N. Papadopoulos, S. Forget, F. Balembois, and P. Georges, "Fluorescence lifetime imaging with a low-repetition-rate passively mode-locked diode-pumped Nd:YVO₄ oscillator," *Opt. Lett.* **30**, 168-170 (2005).
17. F. Brunner, G. J. Sp  hler, J. Aus der Au, L. Krainer, F. Morier-Genoud, R. Paschotta, N. Lichtenstein, S. Weiss, C. Harder, A. A. Lagatsky, A. Abdolvand, N. V. Kuleshov, and U. Keller, "Diode-pumped femtosecond Yb:KGd(WO₄)₂ laser with 1.1W average output," *Opt. Lett.* **25**, 1119-1121 (2000).
18. A. Major, L. Giniunas, N. Langford, A. I. Ferguson, D. Burns, E. Bente, and R. Danielius, "Saturable Bragg reflector-based continuous-wave mode locking of Yb:KGd(WO₄)₂ laser," *J. Mod. Opt.* **49**, 787-793 (2002).
19. A. Courjaud, N. Deguil, and F. Salin, "High power diode-pumped Yb:KGW ultrafast laser," in *OSA Trends in Optics and Photonics (TOPS) 73, Conference on Lasers and Electro-Optics*, OSA Technical Digest (Optical Society of America, Washington DC, 2002), paper CThO3, pp. 501-502.
20. G. Paunescu, J. Hein and R. Sauerbrey, "100-fs diode-pumped Yb:KGW mode-locked laser," *Appl. Phys. B* **79**, 555-558 (2004).
21. A. Major, R. Cisek and V. Barzda, "Development of diode-pumped high average power continuous-wave and ultrashort pulse Yb:KGW lasers for nonlinear microscopy," in *Commercial and Biomedical Applications of Ultrafast Lasers VI*; J. Neev, S. Nolte, A. Heisterkamp, and C. B. Schaffer, eds. SPIE Proc. **6108**, 189-196 (2006).
22. Amplitude Systemes, <http://www.amplitude-systemes.com/>.
23. U. Keller, K. J. Weingarten, F. X. K  rtner, D. Kopf, B. Braun, I. D. Jung, R. Fluck, C. H  nniger, N. Matuschek, and J. Aus der Au, "Semiconductor saturable absorber mirrors (SESAM's) for femtosecond to nanosecond pulse generation in solid-state lasers," *IEEE J. Sel. Top. Quantum Electron.* **2**, 435-453 (1996).
24. H. Hellwig, J. Liebertz, and L. Bohaty, "Exceptional large nonlinear optical coefficients in the monoclinic bismuth borate BiB₃O₆," *Solid State Commun.* **109**, 249-251 (1999).
25. H. Hellwig, J. Liebertz, and L. Bohaty, "Linear optical properties of the monoclinic bismuth borate BiB₃O₆," *J. Appl. Phys.* **88**, 240-244 (2000).
26. Z. Wang, B. Teng, K. Fu, X. Xu, R. Song, C. Du, H. Jiang, J. Wang, and Z. Shao, "Efficient second harmonic generation of pulsed laser radiation in BiB₃O₆ (BIBO) crystal with different phase matching directions," *Opt. Commun.* **202**, 217-220 (2002).
27. T. Harimoto, Y. Takeuchi, M. Fujita, "Spectral properties of second-harmonic generation at 800 nm in a BiB₃O₆ crystal," *Opt. Express* **12**, 811-816 (2004).
28. M. Ghotbi, M. Ebrahim-Zadeh, A. Majchrowski, E. Michalski, and I. V. Kityk, "High-average-power femtosecond pulse generation in the blue using BiB₃O₆," *Opt. Lett.* **29**, 2530-2532 (2004).
29. M. Ghotbi, and M. Ebrahim-Zadeh, "990 mW average power, 52% efficient, high-repetition-rate picosecond-pulse generation in the blue with BiB₃O₆," *Opt. Lett.* **30**, 3395-3397 (2005).
30. D. V. O'Connor and D. Phillips, *Time-Correlated Single Photon Counting* (Academic, New York, 1984).
31. P. A. E. Piunno, J. H. Watterson, C. Wust and U. J. Krull, "Considerations for the quantitative transduction of hybridization of immobilized DNA," *Anal. Chim. Acta*, **400**, 73-89 (1999).

1. Introduction

Optical DNA sensor technology has many potential applications in medicine, environmental monitoring, and pathogen detection, particularly if the sensor device is capable of offering high detection selectivity, sensitivity in addition to reusability and the ability to provide for real-time monitoring [1, 2]. One of the widely used methods of optical DNA detection is based on the measurement of fluorescent lifetimes of selective fluorescent nucleic acid

binding ligands. For example, ethidium bromide is a popular fluorescent label with an absorption band in the green part of the visible spectrum and exhibits a change in fluorescence lifetime from ~1.5-2.0 ns when in solution to ~20-22 ns when intercalatively bound to double-stranded nucleic acid structures [3]. Such drastic lifetime changes can be easily detected and make this dye particularly attractive for use in optical DNA detection techniques.

Rapid and accurate optical interrogation of fluorescence lifetimes of transduction elements associated with the optical biosensor requires a source of pulsed laser radiation with a repetition rate on the order of several megahertz (MHz) and a pulse duration much shorter than the shortest fluorescence decay component of the dye. Widely used free-running dye lasers, however, have extremely low repetition rates (~Hz) and relatively long pulse durations (~ns). On the other hand, femtosecond and picosecond mode-locked solid-state lasers can offer excellent temporal resolution, however, they typically operate with repetition rates on the order of 100 MHz. The pulses at high repetition rate produce excitations in a partially relaxed system and therefore can influence the determination of fluorescence lifetimes. The near-infrared laser emission does not permit for efficient excitation of fluorescent nucleic acid binding ligands, which typically have absorption maxima predominantly in the visible spectral range. Similarly, diode lasers suffer from a bad beam quality, modest average and peak output powers, and are not available in the green wavelength region.

Owing to the high peak powers associated with the ultrashort pulses of solid-state lasers, efficient frequency doubling of the fundamental radiation into the visible part of the spectrum can be produced *via* second harmonic generation in nonlinear crystals. For lasers operating near 1 μm , frequency doubling crystals may be employed to provide for output in the desired range of ~500-540 nm. Two of the most widely used families of solid-state lasers operating near 1 μm are based on Nd^{3+} -ion and Yb^{3+} -ion doped laser materials, such as Nd:YAG or Yb:YAG. Efficient and reliable operation of such ultrashort pulse lasers can be achieved under direct diode-pumping conditions, using laser diodes emitting around 808 and 980 nm, respectively [4].

To overcome the limitation in observable fluorescence lifetime imposed by the high pulse repetition rate (~100 MHz) of the ultrashort pulse lasers, several techniques can be used. Pulse repetition rates can be reduced by an external cavity pulse picker, or intracavity modulator acting as a cavity dumper [5,6]. Both of these methods, however, require high-speed and high-voltage electronics, adding to the complexity and cost of the laser system. Since pulse repetition rate is inversely proportional to the length of a laser resonator, the repetition rate can be reduced by extending the laser cavity. This approach was first implemented with a flash-lamp pumped Nd:glass laser [7], and later successfully used with Ti:Sapphire [8,9], Cr:forsterite [10] and directly diode-pumped lasers [11-14].

In this paper we report on the design and application of a diode-pumped femtosecond extended cavity Yb:KGW laser, which was subsequently frequency-doubled and used as a source for optical DNA sensing. The design proved to be efficient, reliable, power-scalable and provided trouble-free laser operation for months. The main points which determined these features of our laser system came from the following considerations: the use of a Yb:KGW crystal [15] as a laser gain medium instead of, for example, Nd:YAG or Nd:YVO₄, as the Nd-doped crystalline hosts exhibit narrow gain bandwidths and only supports the generation of picosecond pulses [4], therefore reducing temporal resolution. In addition, such lasers usually rely on the use of expensive high-power (> 15-25 W) fiber-coupled laser diode modules. For instance, a high-power picosecond diode-pumped Nd:YVO₄ laser system was recently developed and used for fluorescence lifetime imaging microscopy [16]. On the contrary, the crystal of Yb:KGW can support ~100 fs pulses [17-21] and can be pumped by low-power (~2-4 W) and low-cost telecom-grade long-lifetime multimode laser diodes operating at 970-980 nm (14-pin butterfly package, fiber-coupled, integrated with thermo-electric cooler). Such diode modules, however, are not readily available at 808 nm. The crystal of Yb:KGW has a lower quantum defect, lower pump saturation intensity, and higher stimulated emission cross

section when compared to other quasi-three-level Yb-doped laser materials, such as Yb:YAG: all contributing to the increased laser efficiency [17-21]. It is also worth mentioning, that to the best of our knowledge, low repetition rate operation of a femtosecond Yb:KGW laser pumped by multimode telecom-grade laser diodes has not been reported. Recently, using high-power diode modules (> 20 W) a 10 MHz operation of an Yb:KGW laser system was demonstrated by Amplitude Systemes [22].

2. Experimental setup

To avoid aliasing and cumulative effects in the lifetime measurements, the time (period) between the two successive pulses of excitation has to be 3-5 times longer than the longest component of the fluorescence decay. It is therefore required that the laser source should provide a pulse repetition rate corresponding to a period of at least 60 ns to permit for investigation of the long-lifetime component of ethidium bromide intercalated into double-stranded nucleic acid structures (~ 20 ns) [3].

2.1. Laser cavity design

A schematic of the extended cavity diode-pumped femtosecond Yb:KGW laser is presented in Fig. 1. All mirrors M2-M12 (except for the output coupler M1) were highly reflective (HR, $>99.9\%$) over the 1020-1080 nm wavelength range (Layertec GmbH). The output coupler mirror M1 had a 1.5% transmission over the same wavelength range. The laser resonator design was based on a standard delta-cavity (M1-M6) folded by two flat dichroic mirrors (M3, M4) which, in addition to the HR coating, were also designed for efficient transmission ($>95\%$) of the pump wavelength. Cavity focusing mirrors M2 and M5 had radii of curvature (RoC) of 200 mm and provided a ~ 92 μm cavity mode size (diameter) inside the crystal. The turning angles of mirrors M2 and M5 were kept as small as possible to minimize cavity beam astigmatism.

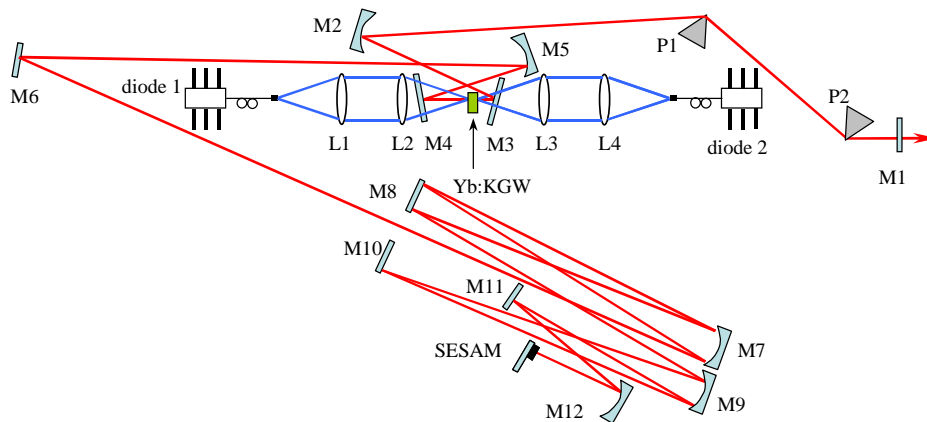


Fig. 1. Schematic design of an extended cavity femtosecond Yb:KGW laser operating at a repetition rate of 15 MHz. Please see text for the details.

In order to reduce the repetition rate of the laser, two identical optical telescopes were incorporated inside the cavity. Each telescope had a 1:1 imaging ratio and was constructed from a concave mirror with $\text{RoC} = 2$ m and plane folding mirrors [8]. The first telescope was made of mirrors M7 (curved) and M8 (flat), and the second one from M9 (curved), and flats M10, M11. This arrangement provided cavity length extension of up to 8 m (or 16 m per cavity round-trip) and resulted in a 15 MHz repetition rate or 67 ns between two consecutive pulses. Therefore, such repetition rate was found suitable for accurate fluorescent lifetime measurements of up to 20 ns (*i.e.* of intercalatively-bound ethidium bromide).

To obtain femtosecond pulse generation, two intracavity dispersive prisms (P1, P2) were used to compensate for the positive dispersion and self-phase modulation introduced by the crystal, glass of prisms and reflections from the cavity mirrors. The prisms were made from SF10 glass (CVI Inc.) and separated by ~38 cm. A semiconductor saturable absorber mirror (SESAM, Batop GmbH) with a specified modulation depth of 1% (non-saturable loss of ~0.5%) was inserted at one end of the cavity and served as a mode locking element [23]. The beam was focused onto a SESAM to a ~100 μm diameter spot by a focusing mirror M12 with a RoC of 150 mm.

The Yb:KGW crystal was a flat/flat 2-mm-thick plate with 5% of Yb-ion doping. It was cut along the Np-axis, such that the laser polarization would be parallel to the high-gain Nm-axis [15]. The crystal's facets were laser grade polished and antireflection coated for the pump and laser wavelengths. The crystal was held in an aluminum housing (without external cooling), which in turn was secured to an xyz-stage to allow for precise alignment. It was slightly tilted against the beam to avoid etalon effects during mode-locked operation.

2.2. Pump diode modules

The Yb:KGW crystal has three strong absorption bands centered around 930 nm, 950 nm and 980 nm [21] which are polarization dependent. The amount of heat generated inside the crystal during laser operation depends on the energy difference between the pump and laser photons (*i.e.* quantum defect) and should be as small as possible to avoid thermal effects, such as thermal lensing. Therefore, pumping at 980 nm (direct excitation of the upper lasing level of the Yb³⁺-ion) is an obvious solution to minimize heat deposition inside the crystal.

Since optical pumping at 980 nm yields the smallest quantum defect, two laser diodes (PhotAura Inc.) operating near this wavelength were used as the pump sources. The output of each laser diode was fiber-coupled into a 1.5 m long multimode fiber with a core diameter of 105 μm and nominal NA of 0.22. The ends of the fibers were terminated with a standard flat-polished SMA905 type connector. Each laser diode was contained in a 14-pin butterfly package (telecom standard) which also included a thermo-electric (Peltier) cooling/heating module, a thermistor for temperature monitoring and feedback control for the Peltier element, and a photodiode for feedback controlled power output. The diodes could provide up to 2.5 W of output power (at the fiber tip) when operated at ~3.6 A of forward current.

The position of the central wavelength could be tuned by varying the temperature of the diodes. The optimum operating temperature was found to be around 40-42 °C and corresponded to a central wavelength of ~978 nm. Temperature tuning of the laser diodes also changed the width of the spectra, where the full width at half-maximum (FWHM) was measured to be in the range of 2.5-4.5 nm. The output radiation exiting the fiber was unpolarized and had a flat-top transverse intensity distribution profile.

The diodes were mounted on brass heat sinks (thermal grease was used to enhance heat transfer efficiency) and were temperature-controlled *via* a feedback loop through the internal thermistor and Peltier element to within a 0.1 °C precision. Water cooling of the heat sinks was not necessary due to small amounts of heat released by the diodes.

To double the amount of available pump power, the laser crystal was longitudinally pumped from both sides (see Fig. 1). The output of the diodes was first collimated by spherical antireflection coated 50 mm focal length lenses (L1, L4) and then refocused by similar lenses (L2, L3) through the dichroic mirrors M3 and M4 into the Yb:KGW laser crystal. Since the lenses were used in a 1:1 imaging configuration, the pump spot size inside the crystal was approximately equal to the fiber core diameter (~105 μm), and therefore closely matched that of the cavity mode size inside the crystal (~92 μm in diameter). This requirement was necessary as the unpumped regions of the crystal (owing to the quasi-three-level laser scheme) have re-absorption at the laser wavelength and therefore act as sources of loss [21].

The total incident pump power onto the crystal was estimated to be close to 4 W (with diode current of ~3.6 A). The pump losses at the conditioning lenses and dichroic mirrors were approximately 10%. It should be noted that the pump losses at the dichroic mirrors sharply increased with the angle of incidence, with the lowest loss (<5%) being at normal incidence. Higher pump losses existed in this system as the dichroic mirrors could not be used at normal incidence due to mechanical constraints.

Approximately 50-60% of the pump was absorbed by the crystal as the pump radiation was not polarized and was not perfectly matched to the peak absorption wavelength of the Yb:KGW. It was also observed that the output power showed a significant dependence on the degree of bending of the diode's fiber. The reason for this is perhaps related to stress-induced birefringence, which can partially polarize the output radiation and lead to higher pump absorption in the crystal.

3. Mode-locking results

Stable mode locking at ~15 MHz repetition rate was achieved using an output coupler (mirror M1) with 1.5% transmission. The pulse repetition period was measured to be 67 ns, as can be seen from the pulse train oscilloscope trace shown in Fig. 2(a). A fast photodiode was used for these measurements (combined resolution of ~1 ns for the photodiode and oscilloscope).

In this configuration, up to 35 mW of average output power was achieved at a pulse repetition rate of 15 MHz. This translates to more than 2 nJ of energy per pulse. The spectrum of the pulse, centered around 1042 nm, is shown in Fig. 2(b) and corresponds to a ~180 fs pulse duration, assuming transform-limited pulses which follow the $sech^2$ of the intensity profile. Second-order autocorrelation measurements based on two-photon absorption in a red light-emitting diode showed that the pulse duration slightly deviates from transform-limited value and is ~200 fs. The peak power delivered by the pulses can be estimated to be 10 kW, which is sufficient for second harmonic generation.

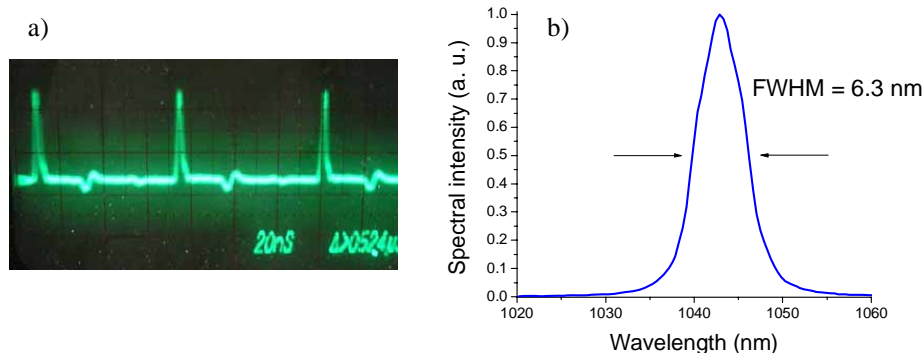


Fig. 2. The train of pulses at 15 MHz measured with a fast photodiode (a) and the optical spectrum of ~200 fs pulses (b).

The energy fluence on the SESAM (with the mode spot diameter of ~100 μm) was calculated to be 1.7 mJ/cm^2 and no damage to the device was observed even after extended operation (months). Passive mode-locking was completely self-starting and could be sustained for many hours of operation, provided that effects of air currents could be avoided by enclosure of the laser in a box.

4. Higher output power setup

As mentioned above, the developed femtosecond Yb:KGW laser provided reliable trouble-free operation for months of constant use. This was achieved by careful selection and optimization of active/passive optical and optomechanical components. Another important

feature of the current design, which was taken into account, is the ease with which the pump diode modules can be replaced or upgraded.

As the employed diode modules were fiber-coupled and terminated with a common connector type (SMA905) that were in turn supported by regular fiber adapters fitting into an optical mount, the replacement of a particular pump module is a simple and straightforward task. The user needs only to replace the fiber-coupled diode laser where, taking advantage of the well-developed telecom components, the replacement fiber tip can be secured in the same spatial location with high accuracy, eliminating the need for time-consuming realignment of the whole laser system.

For example, recently we upgraded the original pump diodes with new units capable of providing approximately twice the amount of power. Each of the two new diodes (Lumics GmbH) could provide up to 3.5-3.7 W of laser radiation at 976-978 nm, depending on the temperature of operation. As these diodes were ordered to have the same telecom-grade design features, a simple replacement of the connectors provided an excellent result: the laser immediately delivered 150 mW of average output power in mode-locked regime (*i.e.* without realignment). The output power did not improve upon further optimization of the laser cavity, confirming that the optimal laser operation conditions were left unchanged by the diode's replacement procedure.

The amount of power reaching the crystal was estimated to be approximately 6 W. Because the pump wavelength did not change, only 50-60% of the pump was absorbed in the crystal. Taking into account the 15 MHz repetition rate, the laser provided up to 10 nJ of energy per pulse corresponding to a five-fold improvement with respect to our previous results. The pulse duration remained as before. It should be noted that generation of pulses with the same energy from a conventional Ti:sapphire laser requires more than double the amount of the absorbed pump power in the laser crystal. Further implementation of active laser crystal cooling by thermoelectric modules or water can reduce the extent of thermal population of the upper levels of the lower Yb³⁺-ion manifold and lead to higher laser efficiency and improved operation. The output power can also be increased by using chirped mirrors for dispersion compensation, which have lower insertion losses than the prisms.

5. Second harmonic generation

Since the absorption band of intercalated ethidium bromide is centered at *ca.* 520 nm, efficient excitation of the dye molecules is possible by frequency-doubling the fundamental (1042 nm) output of the laser. A BIBO nonlinear crystal was selected for second harmonic generation as the effective second-order nonlinearity of this material is higher than that for BBO, LBO, KTP and LiIO₃ crystals [24, 25]. Recently, this fact was experimentally confirmed by frequency-doubling ~35 ps pulses at 1064 nm [26], ~100 fs pulses at 800 nm [27,28] and ~2.4 ps pulses at 800 nm [29]. As generation of femtosecond second harmonic emission in the green spectral region from the ~1 μm fundamental output of the laser by use of a BIBO crystal has not been reported, this work serves to report the first experimental results of this kind.

The second harmonic generation was carried out in a single-pass geometry in a nonlinear BIBO crystal cut for type-I critical phase-matching ($\Theta=167.7^\circ$, $\varphi=90^\circ$) that was antireflection coated for both the fundamental and generated harmonic wavelengths. The thickness of the crystal (0.8 mm) was chosen so as to limit temporal walk-off between the pulses of the fundamental and second harmonic wavelengths to ~150 fs and therefore to keep the duration of the latter in the femtosecond regime (< 250 fs).

The output of the laser was focused into the crystal by a 40 mm focal length lens, with the generated second harmonic re-collimated by use of a similar lens. Both lenses were antireflection coated. To filter out the fundamental wavelength, a standard HR mirror was used that provided 99.9% reflection of the fundamental wavelength and more than 90% transmission of the second harmonic output. The spectrum of the second harmonic laser output at ~520 nm is shown in Fig. 3.

Approximately 0.6 mW of the green radiation was generated for ~30 mW of average fundamental power incident on the crystal, which corresponds to a conversion efficiency of 2%. The peak power of the green pulse was estimated to be ~200 W. It is worth noting that the efficiency of second harmonic generation compares favorably with the recent results of low-MHz high-power picosecond laser system developed for fluorescence lifetime imaging microscopy [16]. It can be significantly improved by using a longer BIBO crystal albeit at the expense of longer 520 nm pulses.

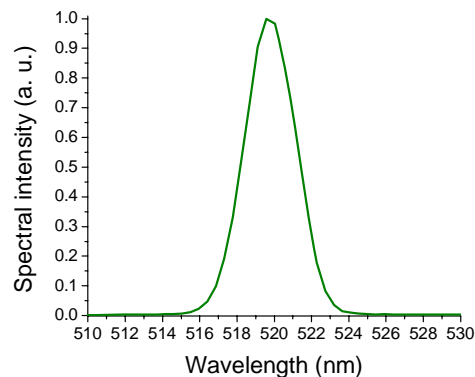


Fig. 3. The spectrum of the second harmonic.

6. Optical DNA detection

The generated second harmonic served as a femtosecond excitation source for the development of an optical DNA biosensor based on fluorescence lifetime measurements by time-correlated single photon counting (TCSPC) [30].

6.1. Fluorescence lifetime measurements

A solution containing 10^{-8} M double-stranded 20-mer oligonucleotides that also contained one equivalent of ethidium bromide was used for all measurements of fluorescence lifetime in our preliminary feasibility studies. This provided for an excess of binding sites capable of supporting intercalative binding of the dye to the double-stranded nucleic acids. The solution was placed in a glass cuvette with 3 mm of path length and excited with the green radiation from the laser. The resultant fluorescence was detected at 90° through the appropriate optical filters (to cut-off scattered pump and background luminescence) by a photomultiplier tube (H5783-20SEL, Hamamatsu), preamplified, and fed to a time-correlated single photon counting device (SPC-630, Becker & Hickl GmbH).

The data collection time was set to a 1 second interval. As shown in Fig. 4, fluorescence lifetimes of ~2 ns (τ_2) and ~20 ns (τ_3) were observed that corresponding to those of well-established values for free and intercalated molecules of ethidium bromide, respectively.

6.2. Optical DNA biosensors

Further experiments using this laser as the excitation source in an optical DNA sensor instrument are currently underway. The design of the optical nucleic acid biosensors is based on an evanescent wave excitation in total internal reflection (TIR) geometry to detect selective binding events of target nucleic acid occurring at the interaction surface of the optical sensors. TIR excitation provides for confined excitation of fluorophores at the chemically selective interface, without excitation of chromophores in the bulk solution. As a result, this approach imparts greater selectivity to the detection scheme by isolation of fluorogenic signals associated only with the reporter dye in the proper environment (as opposed to, for example,

non-selective adsorption events). A diagram of experimental sensor configuration is presented in Fig. 5.

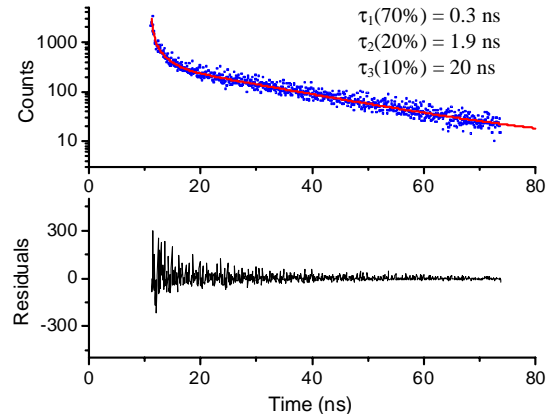


Fig. 4. Test lifetime measurements of ethidium bromide.

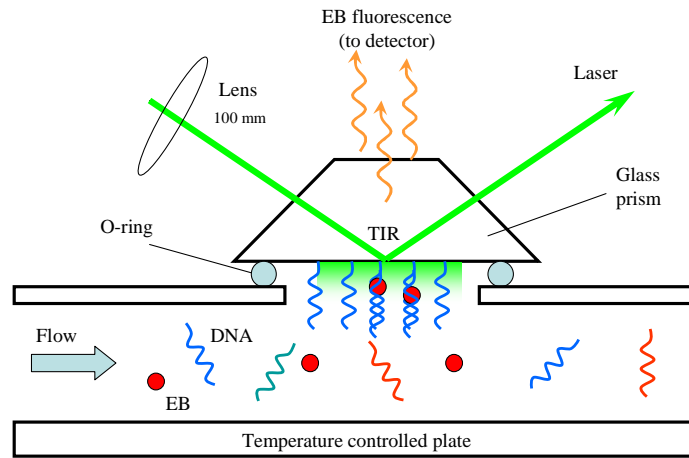


Fig. 5. A diagram of an optical DNA sensor. EB - ethidium bromide.

The sensor's active surface (the base of a fused silica double-coupling prism, $8 \text{ mm} \times 5 \text{ mm} \times 5 \text{ mm}$, $l \times w \times h$) was functionalized [31] with a sequence diagnostic for the neurodegenerative disease spinal muscular atrophy ($5' - \text{ATT TTG TCT AAA ACC CTG T} - 3'$) and exposed to a solution of complementary oligonucleotide and ethidium bromide, each at a concentration of $1 \times 10^{-8} \text{ M}$. Investigations of interfacial nucleic acid hybridization events occurring on the sensor were done by examination of the temperature dependence of the long lifetime component of the fluorescent signal recovered from the optical sensors. This was done by plotting the pre-exponential factor α_3 for the longest lifetime component τ_3 as a function of temperature. At elevated temperatures, thermal denaturation of double-stranded DNA sequences results in release of the intercalated fluorophores, which leads to a subsequent decrease in the observed fluorescence lifetime (from 20 to 2 ns).

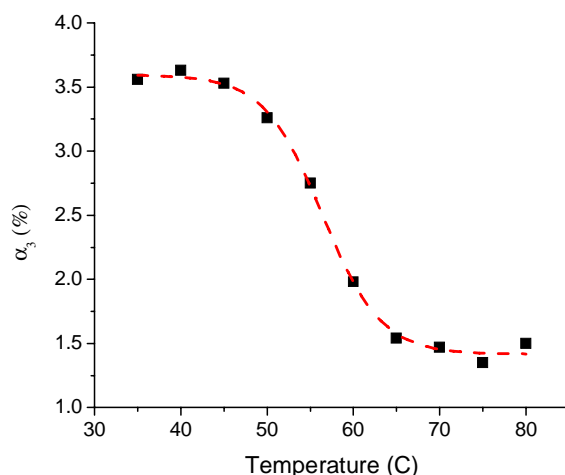


Fig. 6. Thermal denaturation studies of the SMN2 sensor.

As shown Fig. 6, a clear biphasic transition that is consistent with oligonucleotide hybridization/dehybridization was observed and the interfacial duplex melting temperature was estimated to be 57 °C. Four sensors were tested, all showing similar results. A detailed characterization of the optical DNA biosensors will be reported at a later date.

7. Conclusion

We have presented the design, characterization and application of the extended cavity diode-pumped femtosecond Yb:KGW laser passively mode-locked by a semiconductor saturable absorber mirror. The use of high-quality optical and telecom components provided efficient, reliable, power-scalable and trouble-free laser operation for prolonged period of time. The Yb:KGW laser delivered up to 150 mW of average output power with ~200 fs pulses at a repetition rate of 15 MHz, corresponding to a pulse energy of 10 nJ. Frequency-doubled output at 520 nm and low pulse repetition rate made the developed laser an ideal excitation source for the fluorescence lifetime based optical DNA sensor applications.

Acknowledgments

Funding for this project was provided by Genome Canada through the Ontario Genomics Institute, the Ontario Ministry of Agriculture and Food through the Food Safety Research Program, Canada Foundation of Innovation, Ontario Innovation Trust and the Natural Sciences and Engineering Research Council of Canada. The authors would like to acknowledge the help of S.C. Jantzi, C.C. Kotoris and S. Raha with DNA sensor preparation.